DOI: 10.1002/ejic.200900508

# NHTS: A Hollow, Noble-Metal-Modified Titanium Silicalite

Chunfeng Shi,[a] Bin Zhu,[a] Min Lin,*[a] and Jun Long*[a]

**Keywords:** Heterogeneous catalysis / Palladium / Oxidation / Hydrothermal synthesis / Zeolites

The major drawback of direct oxidation technology (onsite hydrogen peroxide production followed by its conversion into organic oxides without refining) is the design and preparation of the bifunctional catalysts used therein. Herein we present a bifunctional catalytic material (NHTS), which is synthesized by a revised semi-in-situ method that allows a noble metal to be distributed throughout the titanosilicate framework and also results in a redistribution of active Ti species throughout the crystals, thereby enriching the surface of the hollow crystals with catalytic species. This compound has been characterized by various techniques and its activity and selectivity for the direct epoxidation of propylene investigated. The results indicate that NHTS shows a very ordered MFI topology, with the noble metal incorporated in the framework, and a hollow structure, which makes it a good alternative for catalytic oxidations.


## Introduction

Microporous crystalline titanium silicalite with an MFI topological structure (i.e. TS-1), whose discovery and application are regarded as milestones in the zeolite and heterogeneous catalysis fields,[1] can catalyze a large number of oxidation reactions with a variety of reactants, such as the conversion of alkanes to alcohols and ketones, secondary alcohols to ketones, secondary amines and ammonia to dialkylhydroxylamines and hydroxylamine,[2,3] as well as alkene epoxidation, phenol oxidation, ketone ammoximation, etc.,[4] using hydrogen peroxide ($H_2O_2$, HP) as oxidant.[5,6] The oxidation of organic substances with HP is regarded as an attractive route for the production of organic oxides since, in contrast to conventional technologies, it does not produce by-products. The transition of key reactions, such as phenol oxidation, ketone ammoximation, and alkene epoxidation, from the laboratory to the factory has either already happened or is likely to happen in the very near future.[7,8]

HP is a versatile and environmentally friendly oxidant.[9] However, as the existing manufacturing processes for HP production are very complex, expensive, and energy-intensive, it is a relatively expensive reagent[10] and price has become an obstacle to the route's commercial acceptance.[11] One of the best ways to reduce this cost is to generate HP in situ from $H_2$ and $O_2$.[12,13] Such a direct HP synthesis process not only has the potential for significant cost savings but also produces an effective, environmentally friendly oxidant without the waste or high costs associated with traditional manufacturing processes.[14] Moreover, a recently developed direct technology involving onsite HP synthesis followed by its conversion into organic oxides without refining (i.e. coupling the direct synthesis of HP from $H_2$ and $O_2$ with the oxidation of reactants in one reaction zone − a one-pot process) is considered to be a very promising technology with huge potential for savings in terms of capital and production costs.[15,16] The key point of this technology is the design and preparation of the catalysts used therein,[17,18] which are bifunctional and mostly consist of a noble metal and titanium silicalite. Noble metals, including platinum, palladium, etc., supported on titanosilicate have been explored as catalysts previously. At present, however, the main difficulty in this process is the efficient preparation of HP in situ − only low $H_2$ and $O_2$ efficiencies are encountered in joint processes,[19] which makes the process economically unviable for the moment. The key to this process therefore involves improving the $H_2$ and $O_2$ efficiencies[20,21] by either preparing new catalysts or reconsidering known catalysts.

One of the best methods for obtaining high yields in oxidation processes involves fast removal of the target oxidation products initially formed in order to avoid their further oxidation into less valuable products (especially fully oxidised products such as $CO_2$ and $H_2O$).[22] In most heterogeneous catalytic oxidations, however, diffusion is the key limiting factor, although this can be overcome by the use of porous catalysts, such as molecular sieves, which allow rapid diffusion of target products out of the catalysts. The presence of micropores in molecular sieves can limit the diffusion of molecules to their internal catalytic sites. Thus, molecular diffusion in catalysts with a hollow structure (with intra-particle voids) is faster than that in a solid

[a] State Key Laboratory of Catalytic Material and Reaction Engineering, Research Institute of Petroleum Processing (RIPP), SINOPEC,
Beijing 100083, P. R. China
Fax: +86-10-82368801
E-mail: chfshi@yahoo.com.cn

  

structure with the same particle size and pore radius due to the greater ease of molecular diffusions to internal active sites.[23,24] One of the aims of our research is to design and prepare porous catalytic materials with such a hollow structure. In recent publications, we have presented a titanosilicate with a hollow structure[23,25] and another with bifunctionality, which we synthesized by a semi-in-situ method[26] and is a hollow titanium silicalite combined with a noble metal (denoted as NHTS). In this work, we re-synthesize NHTS using a revised "semi-in-situ" method (also known as a reprocess method) and present detailed information regarding NHTS, especially in comparison with other samples [including TS-1 and TS-1 with a supported noble metal (Pd/TS-1) prepared using the conventional impregnation method]. The samples were characterized by various analytical techniques, including X-ray fluorescence, powder X-ray diffraction, Fourier transform infrared spectroscopy, UV/Vis diffuse reflectance spectroscopy, X-ray photoelectron spectroscopy, transmission electron microscopy and $N_2$ adsorption-desorption isotherms. Their catalytic performance in the epoxidation of propylene with $H_2$ and $O_2$ as oxidant was also investigated and the differences are discussed herein.

## Results and Discussion

### X-ray Fluorescence (XRF)

The XRF analysis results for NHTS are listed in Table 1 along with those for TS-1 and Pd/TS-1 for comparison. It can clearly be seen that NHTS and Pd/TS-1 contain PdO, $SiO_2$ and $TiO_2$, whereas TS-1 contains only $SiO_2$ and $TiO_2$. Moreover, the $SiO_2$ and $TiO_2$ contents of NHTS and Pd/TS-1 decrease slightly upon introduction of Pd into the titanium silicalite matrix (TS-1), which matches well with what would be expected given the presence of 0.44 and 0.47 wt.-% PdO in NHTS and Pd/TS-1, respectively. There are no great changes in the $TiO_2/SiO_2$ ratio between the semi-in-situ synthesized sample (NHTS) and the conventional impregnated one (Pd/TS-1), which may demonstrate that introduction of the noble metal during the reprocess procedure does not affect the composition of titanium silicalite, in other words, incorporation of Pd into the framework does not alter its chemical composition as the oxide form of titanium silicalite.

Table 1. XRF analysis data, relative crystallinity, and $I_{960}/I_{550}$ values for NHTS, TS-1, and Pd/TS-1.

| Samples | PdO [wt.-%][a] | $SiO_2$ [wt.-%] | $TiO_2$ [wt.-%] | Relative crystallinity [%] | $I_{960}/I_{550}$ |
|---|---|---|---|---|---|
| NHTS | 0.44/0.43 | 97.35 | 2.21 | 105 | 0.696 |
| TS-1 | – | 97.74 | 2.26 | 100 | 0.675 |
| Pd/TS-1 | 0.47/0.31 | 97.30 | 2.23 | 93 | 0.667 |

[a] The first figure is for the fresh catalyst and the second for the recycled catalyst.

### X-ray Diffraction (XRD)

The X-ray diffraction patterns of the samples are shown in Figure 1 (normal patterns are shown on the left and enlargements of the $2\theta$ region between 22 and 25° on the right). The main diffraction peaks for NHTS and Pd/TS-1 are clearly the same as those of the typical titanium silicalite with an MFI topological structure.[27,28] This indicates that the introduction of Pd into the TS-1 framework has no effect on its crystal structure. The relative crystallinities of NHTS and Pd/TS-1 were calculated according to the method described in literature,[29] with TS-1 as standard; the results are listed in Table 1. The relative crystallinity of NHTS increases slightly to 105%, whereas the relative crystallinity of Pd/TS-1 decreases slightly to about 93%. These changes indicate that the different impregnation methods have different effects on the ordering, with the reprocess method increasing the ordering (for NHTS) and the conventional impregnation method decreasing it (for Pd/TS-1). Furthermore, it can be seen that the XRD patterns of NHTS and Pd/TS-1 (Figure 1, parts A and C) show no characteristic signals for pure Pd (simple substance) or PdO species, thus indicating the very high dispersion of Pd species in the titanium silicalite matrix (TS-1).[30,31]

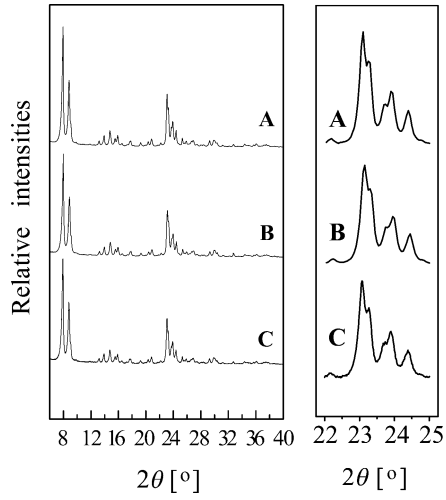


Figure 1. XRD patterns for NHTS (A), TS-1 (B), and Pd/TS-1 (C).

### Fourier Transform Infrared Spectra (FT-IR)

The main absorption bands in the FT-IR spectra of NHTS, TS-1, and Pd/TS-1 (Figure 2) are found at 550, 800, 960, 1100 and 1230 $cm^{-1}$, in agreement with the typical FT-IR spectra of TS-1 reported in the literature.[32] It is well known that an absorption band near 960 $cm^{-1}$ is due to the stretching mode of tetrahedral $SiO_4$ bonded to Ti atoms and is considered to be a fingerprint absorption of framework Ti, especially Ti-containing silicalites.[33,34] The existence of a band at 960 $cm^{-1}$ is always consistent with a low symmetry of the framework structure,[35,36] therefore the decrease in symmetry of the framework structure is indirect evidence for the incorporation of Ti into the MFI struc-

  

ture.[37] In our case, the characteristic "fingerprint" band is clearly detected at around 960 $cm^{-1}$, although for NHTS it is shifted to 967 $cm^{-1}$. This is likely due to the change of the coordination structure resulting from either incorporation of the noble metal in the crystal framework or by the deposition of the noble metal into microporous channels. The peak area ratios for the band at 960 $cm^{-1}$ and that at 550 $cm^{-1}$ for all samples ($I_{960}/I_{550}$ represents the relative Ti content in the framework and can thus represent the symmetry of the framework) are summarized in Table 1, where it can be seen that the peak area ratio for NHTS is slightly higher than that of TS-1 whereas the peak area ratio for Pd/TS-1 is slightly lower. This is in agreement with the ordering suggested by XRD and means that an irreversible change in the framework symmetry of TS-1 occurs upon incorporation of the noble metal and that the change that occurs during the reprocess method (for NHTS) is larger than that which occurs following the conventional method (for Pd/TS-1). These differences are also likely to affect the catalytic performance.

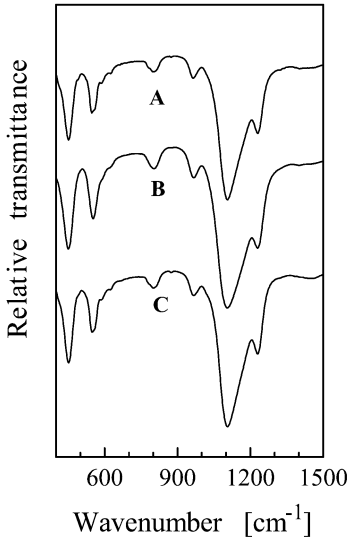


Figure 2. IR spectra for NHTS (A), TS-1 (B), and Pd/TS-1 (C).

## UV/Vis Diffuse Reflectance Spectra (UV/Vis)

The presence of isolated, intra-framework, tetrahedral $Ti^{4+}$ ions was also indirectly verified by UV/Vis spectroscopy (see Figure 3). It is well known that additional evidence for the presence of isolated Ti ions in tetrahedral locations in the silicate lattice can be obtained from the diffuse reflectance UV band, which is indicative of a charge-transfer process from the ligand oxygen to an unoccupied orbital of the central Ti ion in isolated $Ti(OSi)_4$ or $Ti(OSi)_3$-(OH) units.[38] Figure 3 (A) shows that NHTS gives only one strong UV absorption band at 210 nm, thus indicating the existence of isolated, intra-framework, tetrahedral $Ti^{4+}$ ions only, whereas TS-1 and Pd/TS-1 give UV absorption bands (Figures 3, B and C) at 210 (strong band) and 330 nm (a mild one), which clearly shows the existence of both isolated, intra-framework, tetrahedral $Ti^{4+}$ ions and extra-framework anatase-type $TiO_2$ in TS-1 and Pd/TS-1. Moreover, the absorption intensities of the intra- and extra-framework bands are almost the same before introduction of the noble metal and afterwards, thus indicating that the introduction of a noble metal by the conventional impregnation method does not severely affect the framework Ti structure of titanium silicalite. The framework is very stable under such conditions, even when undergoing impregnation with the noble metal, washing with deionized water and calcination at high temperature. However, the reprocess procedure also affects the coordination of Ti by avoiding the formation of extra-framework Ti, thereby ensuring that essentially all the $Ti^{4+}$ ions in NHTS have a tetrahedral coordination (intra-framework). A single broad absorption band centered at around 485 nm, assigned to the absorption of noble metal species,[39] also appears in theUV/Vis spectra of NHTS and Pd/TS-1 (Figures 3, A and C), thus confirming the incorporation of noble metal species into NHTS and Pd/TS-1 and therefore the above XRD analysis.

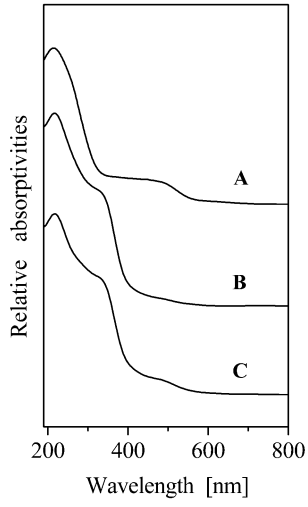


Figure 3. UV/Vis spectra for NHTS (A), TS-1 (B), and Pd/TS-1 (C).

## X-ray Photoelectron Spectra (XPS)

The main XPS Pd 3d peak for Pd particles or foils appears at a binding energy (BE) of 335.0 eV, while for PdO this peak appears at a BE of 336.8 eV.[40,41] The XPS Pd 3d peaks for NHTS and Pd/TS-1 (Figures 4, A and B) appear at 335.3 and 335.6 eV, respectively. In order to help the understanding of our readers, we have fitted the Pd 3d spectra shown in Figure 4 to two doublets − one belonging to Pd metal and the other to PdO − as this allows us to determine the true BE values and proportion of each species more precisely. The fitted figure shows that the peak area ratio of Pd metal and Pd metal oxide is about 5:3 and 3:2 for NHTS and Pd/TS-1, respectively. These values suggest that the state of Pd in NHTS and Pd/TS-1 is most likely a simple substance state mixed with a small amount of oxide state, in other words the states are neither a pure simple substance

  

state nor a pure oxide one. This further indicates the presence of interactions between the metal and the titanium silicalite matrix and that these interactions alter the microstructure, especially the electronic structure of Pd.[26] These changes would affect the catalytic performance in propylene epoxidation.

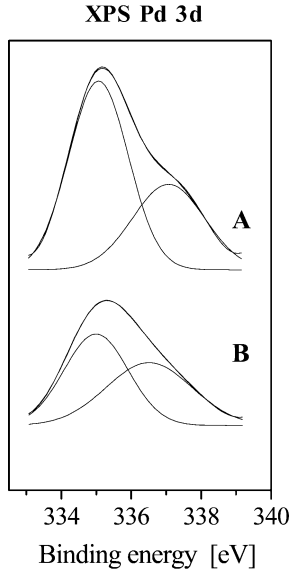


Figure 4. XPS Pd 3d spectra for NHTS (A) and Pd/TS-1 (B).

The detection of octahedral and tetrahedral Ti ions by XPS analysis is a common analytical technique − the tetrahedral Ti 2p 3/2 peak is usually found at a BE of 460.0 eV whereas the octahedral Ti 2p 3/2 peak is found at a BE of 458.0 eV.[42,43] In order to better visualize the spectra and to allow us to get more reliable information concerning the state of the $Ti^{4+}$ ions and to quantify the proportion of tetrahedral and octahedral $Ti^{4+}$ species, we also fitted the Ti 2p 3/2 spectra to two doublets − one belonging to tetrahedrally coordinated titanium species and the other to octahedrally coordinated titanium species. The fitted XPS Ti 2p spectra of NHTS, TS-1, and Pd/TS-1 are shown in Figure 5, where it can be seen that NHTS has only one Ti 2p 3/2 peak at a BE of about 460.0 eV. This means that NHTS has only tetrahedrally coordinated titanium species whereas TS-1 and Pd/TS-1 have both octahedrally and tetrahedrally coordinated titanium species (two Ti 2p 3/2 peaks with BEs of about 458.0 and 460.0 eV, respectively). The ratio of octahedrally to tetrahedrally coordinated Ti species, as calculated from the peak area ratio, are approximately 0, 0.8, and 1.0 for NHTS, TS-1, and Pd/TS-1, respectively. The ratios for TS-1 and Pd/TS-1 show that the amount of tetrahedrally coordinated Ti species in Pd/TS-1 is lower than that in TS-1. All these observations are in agreement with the UV/Vis spectral analysis, which suggests that the introduction of Pd by the conventional impregnation method affects the framework Ti structure of titanium silicalites by decreasing the number of tetrahedrally coordinated Ti species (for Pd/TS-1) whereas the reprocess procedure (for NHTS) affects the Ti coordination, thereby ensuring that the Ti species in NHTS are almost all intra-framework species (and therefore have a tetrahedral configuration).

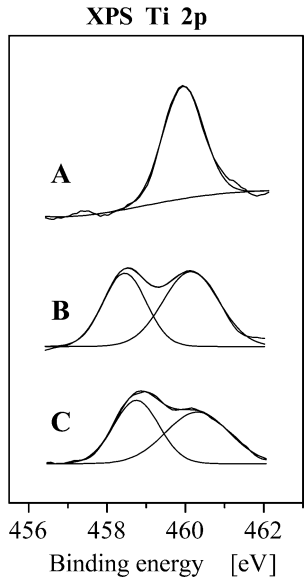


Figure 5. XPS Ti 2p spectra for NHTS (A), TS-1 (B), and Pd/TS-1 (C).

### Transmission Electron Microscopy (TEM)

The representative TEM images of NHTS, TS-1, and Pd/TS-1 shown in Figure 6 (Figures 6, $A_2$, B, and C) show that particles of all samples are highly crystalline with an average crystal size of 0.1–0.3 μm. As can be seen from this figure, the majority of NHTS particles are hollow (Figure 6, $A_2$, many rectangular voids formed in each particle). This demonstrates that the reprocess procedure introduces Pd into NHTS and also results in the formation of intra-particle voids, which means that NHTS has both micro- and mesopores. TS-1 and Pd/TS-1, on the other hand, have a

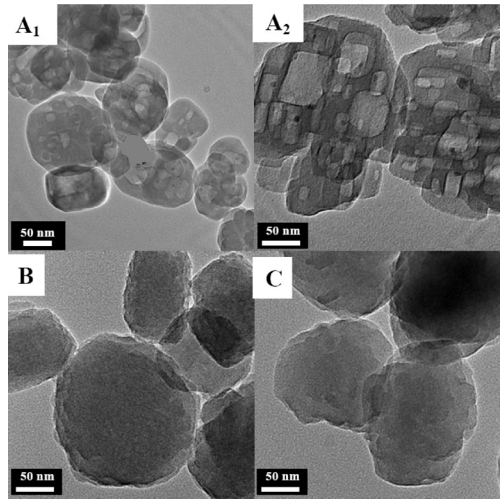


Figure 6. TEM images of NHTS (5 h; $A_1$), NHTS ($A_2$), TS-1 (B), and Pd/TS-1 (C).

  

solid structure (Figure 6, B and C, with micropores), which means that the conventional impregnation method does not affect the morphology of the intra-particle voids in TS-1. These findings were confirmed by $N_2$ adsorption-desorption isotherms (see below). Furthermore, the TEM images in Figures 6 ($A_2$ and C) confirm that NHTS and Pd/TS-1 show no obvious particles of pure Pd (simple substance) or PdO species, thereby indicating that, at relatively low Pd contents, both the semi-in-situ and conventional impregnation methods result in a very high dispersion of Pd species in the titanium silicate matrix, in agreement with the XRD results.[44,45]

### $N_2$ Adsorption-Desorption Isotherms

The $N_2$ adsorption-desorption isotherms of NHTS, TS-1, and Pd/TS-1 are shown in Figure 7. NHTS (Figure 7, A) shows a typical type IV adsorption-desorption curve (according to the IUPAC classification) with an obvious hysteresis loop in the isotherm, thus suggesting that NHTS has a hollow structure.[23,25] The isotherms for TS-1 and Pd/TS-1 (Figure 7, B and C), in contrast, are typical type II adsorption curves, which means that they both have a solid structure (with only micropores). These results also confirm that the reprocess procedure results in the both the incorporation of Pd into NHTS and the creation of intra-particle voids, thereby confirming the results of the TEM analysis. The results for all three samples, including the BET specific area and cumulative pore volume, are listed in Table 2, where it can be seen that the incorporation of Pd into the framework using different methods (reprocess method and conventional impregnation) results in different porous parameters. Thus, the BET surface area and pore volume of NHTS (reprocess method) are 424 $m^2 g^{-1}$ and 0.32 $cm^3 g^{-1}$, respectively, whereas for Pd/TS-1 (conventional impregnation method) and TS-1 (not modified by noble metal) they are 389 and 412 $m^2 g^{-1}$ and 0.21 and 0.24 $cm^3 g^{-1}$, respectively. This means that the surface area and pore volume decrease after the incorporation of Pd into the titanium silicalite framework by the conventional impregnation method (for Pd/TS-1). This decrease corresponds to that in the corresponding microporous segments. In contrast, an increase in surface area and pore volume is found for NHTS (compared with TS-1), and this increase corresponds almost exactly to formation of the mesopores (subtracting the parts corresponding to the micropores from the total surface area or pore volume). This means that the hollow structure formed in NHTS has a greater capacity to accommodate extraneous molecules than a solid one, which could affect its catalytic performance.

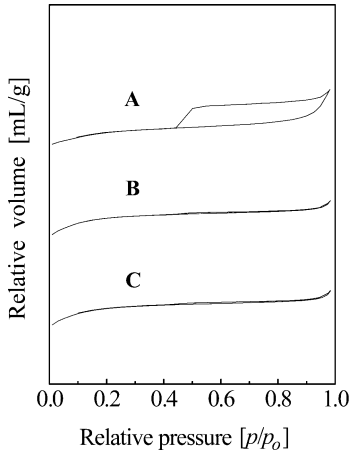


Figure 7. $N_2$ adsorption/desorption isotherms for NHTS (A), TS-1 (B), and Pd/TS-1 (C).

Table 2. Pore parameters and epoxidation catalyst performance for NHTS, TS-1, and Pd/TS-1.

| Samples | Surface area [$m^2 g^{-1}$] | | Pore volume [$cm^3 g^{-1}$] | | $C_{PO}$[a] [wt.-%] | $S_{PO}$[a] [mol-%] |
|---|---|---|---|---|---|---|
| | $S_{Mic}$[b] | BET | $V_{Mic}$[b] | Total | | |
| NHTS | 381 | 424 | 0.17 | 0.32 | 2.5/2.3 | 95.1/92.4 |
| TS-1 | 389 | 412 | 0.18 | 0.24 | – | – |
| Pd/TS-1 | 368 | 389 | 0.16 | 0.21 | 0.9/0.3 | 73.4/65.6 |

[a] The first figure is for the fresh catalyst and the second for the recycled catalyst (used twice). [b] Microporous part.

### Catalytic Epoxidation Results

The catalytic epoxidation properties of TS-1, Pd/TS-1, and NHTS are listed in Table 2, where it can be seen that TS-1 has no catalytic activity under the reaction conditions used whereas NHTS and Pd/TS-1 exhibit good activity. The catalytic activity ($C_{PO}$) is 2.5% for NHTS and 0.9% for Pd/TS-1 and the selectivity ($S_{PO}$) is 95.1% for NHTS (the other products are 1,2-propanediol and two types of methoxypropanol), whereas that for Pd/TS-1 is 73.4% (the other products are the same as for NHTS). These figures show that NHTS is a better epoxidation catalyst than Pd/TS-1. Furthermore, a contrast catalytic experiment with TS-1 with the appropriate amount of commercial HP added was performed, and the positive results provide valuable information regarding the direct epoxidation process. Similarly, the formation of HP from $H_2$ and $O_2$ under our reaction conditions was proven in a separate experiment without addition of propylene, therefore it can be deduced that the formation of HP occurs over the Pd particles whereas propylene epoxidation occurs over the Ti species in the framework.[26] It is likely that the limiting step in this reaction is the formation of HP from $H_2/O_2$ on Pd, which would nicely explain why TS-1 has no catalytic activity (it has no Pd, therefore HP cannot be synthesized in situ from $H_2 + O_2$). Moreover, Pd particles alone have no catalytic activity since they cannot epoxidize propylene to PO in the absence of Ti species. In contrast, both NHTS and Pd/TS-1 have catalytic activity since they both contain Pd and Ti species, which may provide further evidence that this direct process involve HP production in situ followed by its conversion into target organic oxides (mainly PO). The catalyst-recycling results, which are also listed in Table 2, show that the activity of NHTS decreases only slightly ($C_{PO}$ drops from 2.5 to 2.3%)

  

with almost the same high selectivity ($S_{PO}$ drops from 95.1 to 92.4%) whereas the activity of Pd/TS-1 decreases sharply ($C_{PO}$ drops from 0.9 to 0.3%), as does the selectivity ($S_{PO}$ drops from 73.4 to 65.6%), after being reused twice. These results show that most of the catalytic activity and selectivity of NHTS is maintained, whereas the activity and selectivity of Pd/TS-1 drop more rapidly, in other words the catalytic activity and selectivity of NHTS are better than those of Pd/TS-1. The above catalytic results show that NHTS is an excellent catalyst for the production of PO in a one-pot process that couples the direct synthesis of HP from $H_2$ and $O_2$ with the epoxidation of propylene in a single reaction. The better performance of the NHTS catalyst is due to the lower stability of Pd/TS-1 in the epoxidation reaction (metal leaching). Despite the fact that the coordination state of the catalysts does not change (as confirmed by UV and XPS), metal leaching from the spent Pd/TS-1 catalyst was found. The metal contents for the spent catalysts are listed in Table 1, where it can be seen that the Pd content for the spent NHTS catalyst remains essentially unchanged (drops from 0.44 to 0.43) whereas that of the spent Pd/TS-1 catalyst decreases from 0.47 to 0.31. These differences may be a result of the preparation conditions (reprocess procedure, semi-in-situ synthesis), which results in the introduction of stable Pd particles into NHTS and the formation of a hollow structure that facilitates molecular diffusion; all of these factors are likely to affect the catalytic performance. In order to verify this explanation, we performed the reaction between propylene and HP in the absence of $H_2/O_2$ and the reaction between $H_2$ and $O_2$ under the same conditions but without propylene. As reported previously,[46] the first reaction proceeded rapidly under our conditions in the presence of regular TS-1, thus showing that the original (reprocess) method produces a more active and selective titanosilicate. The second experiment confirmed the ability of the Pd component to produce HP. These results (not given here) therefore show that our method produces a more active and selective titanium silicalite than the conventional impregnation method. The Pd component in NHTS is also more active in HP production than that in Pd/TS-1.

### "Semi-in-situ" Synthesis of NHTS

The reason for calling this treatment a reprocess, or semi-in-situ, synthesis is easily illustrated by a simplified scheme (see Scheme 1). The Si, Ti, and Pd sources, etc. are not added in the same step and the Pd source used therein is not the final active Pd species, therefore calling the whole synthetic process a "semi-in-situ"[26] one is accurate. It can clearly be seen from this scheme that the role of the surfactant (CTAB) is as a protective agent to avoid aggregation of the noble metal particles produced by the reducing agent ($N_2H_4{\cdot}H_2O$), thereby guaranteeing the high dispersion of these species into the NHTS framework during the reprocessing step (as demonstrated by XRD and TEM). The large intra-particle voids inside the NHTS crystals, which decrease the pore diffusion limitations and facilitate molecular transport to the catalytic sites, are formed during the dissolution-recrystallization stage (as illustrated by TEM and $N_2$ adsorption-desorption isotherms).[23] Due to the importance of the hollow structure of the NHTS particles, much more consideration was given to their formation mechanism, therefore to describe this mechanism in more detail, we determined an intermediate structure by TEM (Figure 6, $A_1$) after a shorter recrystallization time (5 h). This image suggests that the dissolution process mainly dissolves the particles' cores (each particle is formed from aggregated nanocrystals and therefore has multiple cores) due to their lower crystallinity than the external shell, as also found by Wang et al.[23] Moreover, the hollow structure of the particles in NHTS seems to differ from the hollow nanoporous zeolite single crystals (ZSM-5 nanoboxes with uniform intracrystalline hollow structures),[24] which are capsule-like, probably because NHTS is a new type of titanium silicalite with bifunctionality whereas the other materials[23] are pure silicon-based molecular sieves or aluminium silicalite-based molecular sieves (ZSM-5). Moreover, in analogy to the hollow TS-1 crystals formed previously via a dissolution-recrystallization process,[23] NHTS has many rectangular pores in each particle. The dissolution-recrystallization reprocess performed during the synthesis of NHTS can form intra-particle voids, which results in removal of some of the Ti and Si species from the framework in the intermediate and their subsequent dissolution (they are mainly dissolved from the particles' core, as discussed above).[24] This means that the solution contains Ti, Si, and Pd species (added in this step) at this point. Before the hydrothermal treatment step in the reprocess, these species are enriched at the surface of the intermediate due to the capillary action in this intermediate and, due to the presence of the protective agent (surfactant CTAB), noble metal particles, or species produce upon reduction by the reducing agent ($N_2H_4{\cdot}H_2O$), become highly dispersed on the surface of intermediate. During the reprocess step, however, these species form NHTS (with an MFI topological structure), in the presence of the template agent (TPAOH), during the recrystallization process under reaction conditions analogous to those used for the hydrothermal synthesis of pure silicon ZSM-5 or TS-1 molecular sieves whilst at the same time stably incorporating noble metal species into the framework. It should be noted that, during the whole semi-in-situ procedure (dissolution-recrystallization reprocess), but especially in the later stages, the dissolution and recrystallization processes are conducted simultaneously. The later stages of this reaction are a dynamic and balancing process. Indeed, this semi-in-situ reaction, which includes partial dissolution and recrystallization of the intermediate (titanium silicalite material) during the synthesis of NHTS, both combines a noble metal with the titanosilicate framework and does so stably and modifies the distribution of active Ti species throughout the crystals,[23] thereby enriching the surface of these hollow crystals with catalytic species (both Pd species and Ti species). All these factors are likely to affect the catalytic performance.

  

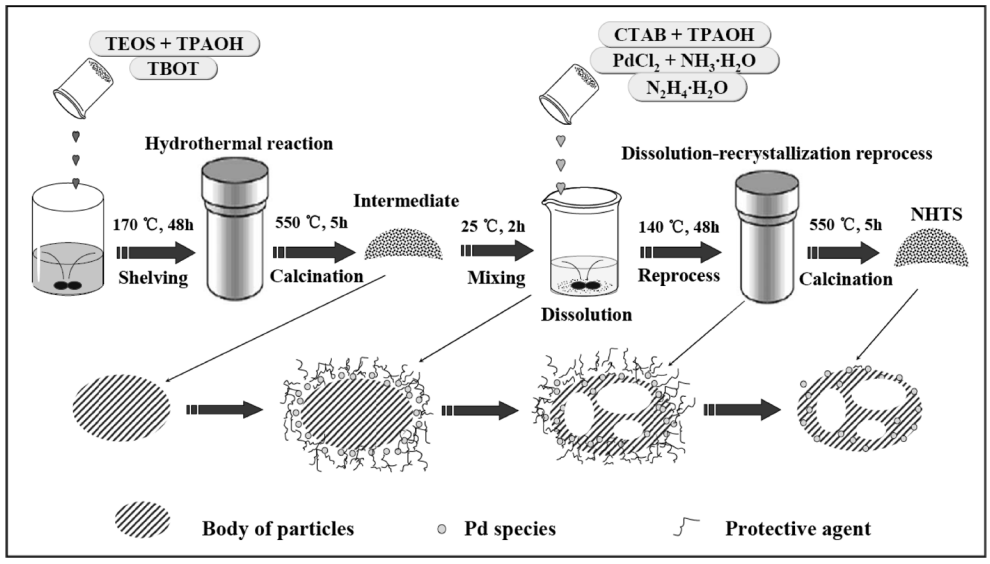


Scheme 1. Simplified scheme showing the "semi-in-situ" synthesis of NHTS, including the reprocess, the introduction of Pd species, and the formation of intra-particle voids.

## Conclusions

NHTS, a new hollow titanium silicalite with a noble metal incorporated into the framework, has been obtained by a semi-in-situ synthetic method, which involves the addition of a noble metal source to the reaction mixture and isolation of an intermediate product under organic-alkaline conditions. This revised semi-in-situ process results in incorporation of the noble metal into the titanosilicate framework and the redistribution of active Ti species throughout the crystals, thereby enriching the surface of the hollow crystals with catalytic species. The characterization results suggest that the as-synthesized NHTS shows a very ordered MFI topology and is a good catalyst for the direct epoxidation of propylene with high selectivity. The catalyst is easily separated and recycled and may therefore find industrial applications.

## Experimental Section

**Materials:** Tetraethyl orthosilicate (TEOS), tetrapropylammonium hydroxide (TPAOH, 25 wt.-% in $H_2O$), tetrabutyl orthotitanate (titanium butoxide, TBOT), 2-propanol, hexadecyltrimethylammonium bromide (CTAB), ammonia ($NH_3{\cdot}H_2O$, 30 wt.-% in $H_2O$), palladium chloride ($PdCl_2$), hydrazine hydrate ($N_2H_4{\cdot}H_2O$, 85 wt.-% in $H_2O$), hydrogen peroxide ($H_2O_2$, 30 wt.-% in $H_2O$), and methanol (all analytical grade) were purchased from Beijing Chemical Co. (China), as were propylene (polymer grade) and $N_2$, $O_2$, and $H_2$ (99.995 vol.-%).

**Synthesis:** NHTS was synthesized following a slightly modified semi-in-situ procedure (herein the reprocess method) described in the literature.[26] Thus, 42 g of TEOS was thoroughly mixed with 14.5 g of TPAOH solution and 110 g of distilled water. Subsequent hydrolysis at 75 °C for 3 h gave a hydrolyzed TEOS solution, to which a solution composed of 1.3 g of TBOT and 8.5 g of anhydrous 2-propanol was added slowly with stirring. The mixture obtained was stirred at 75 °C for 3 h and then transferred to a stainless steel autoclave, which was heated under autogenous pressure at 170 °C for 2 d. The resultant mixture of crystallization products was filtered, washed with distilled water, dried at 120 °C for 5 h, and calcined at 550 °C in air for 5 h, to give the intermediate product. This product obtained was then mixed with TPAOH and a CTAB solution containing $PdCl_2$ and $NH_3{\cdot}H_2O$ in an intermediate product (g)/TPAOH (mol)/CTAB (mol)/$PdCl_2$ (g)/$NH_3{\cdot}H_2O$ (mol)/water (mol) ratio of 100:1.0:0.1:2.0:1.0:25. After stirring for 2 h, the appropriate amount of $N_2H_4{\cdot}H_2O$ was added to the mixture, which was then transferred to an autoclave and the reprocess procedure carried out under autogenous pressure at 140 °C for 48 h. After cooling and pressure release, subsequent filtration, washing, drying, and calcination gave NHTS. Before characterization and testing, the product was heated from room temperature to 150 °C under pure $N_2$, at a rate of 2 K $min^{-1}$, and kept at that temperature for 3 h. The catalyst may be auto-reduced under these conditions by thermal decomposition of the $NH_3$ ligands.[47]

For comparison, TS-1 molecular sieves and TS-1 with a supported noble metal (Pd) were also synthesized.

TS-1 molecular sieves were prepared according to the procedure described by Thangaraj et al.[48] Thus, 22.5 g of TEOS was thoroughly mixed with 7.0 g of TPAOH solution and 59.8 g of distilled water. Subsequent hydrolysis at 60 °C for 1.0 h gave a hydrolyzed TEOS solution, to which a solution containing 0.8 g of TBOT and 4.2 g of anhydrous 2-propanol was added slowly with vigorous stirring. The mixture obtained was stirred at 75 °C for 3 h to obtain a clear, transparent colloid, then transferred into a stainless steel autoclave and heated under autogenous pressure at 170 °C for 6 d. The resulting crystallization products were filtered, washed with distilled water to a pH of 8–9, dried at 120 °C for 5 h, and then calcined at 550 °C in air for 5 h to give the required TS-1 molecular sieves.

TS-1 molecular sieves with incorporated Pd (Pd/TS-1) were synthesized according to the conventional impregnation method.

**Characterization:** The Pd content, and that of other elements, in the samples was determined by X-ray fluorescence (XRF) analysis using a Rigaku 3271E X-ray fluorescence spectrometer. Powder X-ray diffraction (XRD) data were recorded with a Siemens D5005

  

(30 kV, 30 mA) using nickel-filtered Cu-$K_\alpha$ radiation; diffraction patterns were collected under ambient conditions in the $2\theta$ range 4–40°. FT-IR spectra were recorded in vacuo, and at ambient temperature, with a Nicolet 8210 infrared spectrometer in the range 400–1600 $cm^{-1}$ using KBr pellets. The diffuse reflectance UV/Vis spectra were obtained with a Perkin–Elmer Lambda 20 UV/Vis spectrometer. X-ray photoelectron spectra were recorded with a PHI Quantera scanning X-ray microprobe (SXM) instrument in vacuo at ambient temperature. TEM experiments were performed with a Tecnai $G^2$F20S-TWIN electron microscope with an acceleration voltage of 300 kV. The nitrogen isotherms at the temperature of liquid nitrogen were measured using a micromeritics ASAP 2010M system.

**Catalytic Test:** Epoxidation of propylene with $H_2$ and $O_2$ as oxidant was carried out in a stainless-steel autoclave equipped with a Teflon® beaker and an electric stirrer. In a typical experiment, the reactor was charged with 1.0 g of catalyst, 40 g of methanol, and 2 g of deionized water. After addition of propylene to a pressure of 0.8 MPa, the vessel was continuously pressurized with hydrogen and oxygen (molar ratio 1:1) until the pressure reached 2.0 MPa. The slurry was heated from room temperature to 40 °C under pressure and vigorous stirring, kept at 40 °C for 1 h, and then cooled down to below 10 °C. At the end of the reaction, the catalyst was filtered off (and reused after drying). Analysis of the liquid phase was performed with an Agilent 6890N gas chromatograph coupled to a flame ionization detector (FID) and a 30-meter FFAP capillary column. As the main product here is propylene oxide (PO), the PO concentration ($C_{PO}$, determined with respect to an external standard) and PO selectivity ($S_{PO}$) were calculated based on the amount of propylene oxide (mol-%) in the products (as also determined with respect to an external standard).

## Acknowledgments

We are grateful for financial support from the of the Ministry of Science and Technology, P. R. China (State Basic Research Project "973", grant no. 2006CB202508) and the China Petrochemical Corporation (SINOPEC) (grant no. S206005). The authors would also like to thank Profs. X. T. Shu, X. Q. Wang, J. Fu, X. H. Mu, and Y. B. Luo from the Research Institute for Petroleum Processing (China) for their helpful suggestions.

[1] W. F. Hölderich, *Stud. Surf. Sci. Catal.* **1989**, *49*, 69–83.
[2] G. N. Vayssilov, *Catal. Rev. Sci. Eng.* **1997**, *39*, 209–251.
[3] A. Zecchina, S. Bordiga, G. Spoto, A. Damin, G. Berlier, F. Bonino, C. Prestipino, C. Lamberti, *Top. Catal.* **2002**, *21*, 67–78.
[4] W. Fan, R. Duan, T. Yokoi, P. Wu, Y. Kubota, T. Tatsumi, *J. Am. Chem. Soc.* **2008**, *130*, 10150–10164.
[5] A. Thangaraj, R. Kumar, P. Ratnasamy, *J. Catal.* **1991**, *131*, 294–297.
[6] D. R. C. Hubrechts, Ph. L. Buskens, P. A. Jacobs, *Stud. Surf. Sci. Catal.* **1992**, *72*, 21–31.
[7] M. G. Clerici, P. Ingallina, *J. Catal.* **1993**, *140*, 71–83.
[8] P. Carlo, C. Angela, I. Patrizia, A. M. Maria, B. Giuseppe, *Appl. Catal. A: Gen.* **2001**, *221*, 63–72.
[9] A. Thangaraj, S. Sivasanker, P. Ratnasamy, *J. Catal.* **1991**, *131*, 394–400.
[10] Y. Han, J. H. Lunsford, *J. Catal.* **2005**, *230*, 313–316.
[11] D. P. Dissanayake, J. H. Lunsford, *J. Catal.* **2002**, *206*, 173–176.
[12] D. P. Dissanayake, J. H. Lunsford, *J. Catal.* **2003**, *214*, 113–120.
[13] W. Laufer, R. Meiers, W. Hölderich, *J. Mol. Catal. A* **1999**, *141*, 215–221.
[14] P. P. Olivera, E. M. Patrito, H. Sellers, *Surf. Catal.* **1994**, *313*, 25–40.
[15] Q. Chen, E. J. Beckman, *Green Chem.* **2008**, *10*, 934–938.
[16] Z. Xi, N. Zhou, Y. Sun, K. Li, *Science* **2001**, *292*, 1139–1141.
[17] T. A. Nijhuis, T. Visser, B. M. Weckhuysen, *Angew. Chem. Int. Ed.* **2005**, *44*, 1115–1118.
[18] N. Yap, R. P. Andres, W. N. Delgass, *J. Catal.* **2004**, *226*, 156–170.
[19] Q. Chen, E. J. Beckman, *Green Chem.* **2007**, *9*, 802–808.
[20] L. Cumaranatunge, W. N. Delgass, *J. Catal.* **2005**, *232*, 38–42.
[21] G. Mul, A. Zwijnenburg, B. Linden, M. Makkee, J. A. Moulijn, *J. Catal.* **2001**, *201*, 128–137.
[22] P. Ratnasamy, D. Srinivas, H. Knözinger, *Adv. Catal.* **2004**, *48*, 1–169.
[23] Y. Wang, M. Lin, A. Tuel, *Microporous Mesoporous Mater.* **2007**, *102*, 80–85.
[24] Y. Wang, A. Tuel, *Microporous Mesoporous Mater.* **2008**, *113*, 286–295.
[25] M. Lin, X. T. Shu, X. Q. Wang, B. Zhu, *US Pat. 6475465*, **2002**.
[26] C. Shi, B. Zhu, M. Lin, J. Long, *Eur. J. Inorg. Chem.* **2009**, 3067–3070.
[27] E. Duprey, P. Beaunier, M.-A. Springuel-Huet, F. Bozon-Verduraz, J. Fraissard, J.-M. Manoli, J.-M. Brégeault, *J. Catal.* **1997**, *165*, 22–32.
[28] M. Taramasso, G. Perego, B. Notari, *US Pat. 4410501*, **1983**.
[29] M. Lin, X. T. Shu, X. Q. Wang, B. Zhu, *CN Pat. 1089279C*, **2002**.
[30] C. Shi, R. Wang, G. Zhu, S. Qiu, J. Long, *Eur. J. Inorg. Chem.* **2006**, 3054–3060.
[31] C. Shi, R. Wang, G. Zhu, S. Qiu, J. Long, *Eur. J. Inorg. Chem.* **2005**, 4801–4807.
[32] P. Fejes, J. B. Nagy, J. Halász, A. Oszkó, *Appl. Catal. A: Gen.* **1998**, *175*, 89–104.
[33] G. Ricchiardi, A. Damin, S. Bordiga, C. Lamberti, G. Spanò, F. Rivetti, A. Zecchina, *J. Am. Chem. Soc.* **2001**, *123*, 11409–11419.
[34] P. F. Henry, M. T. Weller, C. C. Wilson, *J. Phys. Chem. B* **2001**, *105*, 7452–7458.
[35] C. Lamberti, S. Bordiga, A. Zecchina, A. Carati, A. N. Fitch, G. Artioli, G. Petrini, M. Salvalaggio, G. L. Marra, *J. Catal.* **1999**, *183*, 222–231.
[36] G. L. Marra, G. Artioli, A. N. Fitch, M. Milanesio, C. Lamberti, *Microporous Mesoporous Mater.* **2000**, *40*, 85–94.
[37] M. C. Capel-Sanchez, J. M. Campos-Martin, J. L. G. Fierro, *Appl. Catal. A: Gen.* **2003**, *246*, 69–77.
[38] M. R. Boccuti, K. M. Rao, A. Zecchina, G. Leofanti, G. Petrini, *Stud. Surf. Sci. Catal.* **1989**, *48*, 133–144.
[39] V. N. Shetti, P. Manikandan, D. Srinivas, P. Ratnasamy, *J. Catal.* **2003**, *216*, 461–467.
[40] V. R. Choudhary, A. G. Gaikwad, S. D. Sansare, *Catal. Lett.* **2002**, *83*, 235–239.
[41] Y. Hasegawa, A. Ayame, *Catal. Today* **2001**, *71*, 177–187.
[42] D. T. On, L. Bonneviot, A. Bittar, A. Sayari, S. Kaliaguine, *J. Mol. Catal.* **1992**, *74*, 233–246.
[43] V. Arca, A. B. Boscoletto, N. Fracasso, L. Meda, G. Ranghino, *J. Mol. Catal. A* **2006**, *243*, 264–277.
[44] C. Shi, M. Xin, R. Wang, Y. Xie, L. Hu, L. Xu, R. Zhang, G. Zhu, S. Qiu, *Chem. J. Chin. Univ.* **2005**, *26*, 1198–1201.
[45] C. Shi, L. Wan, R. Wang, J. Long, G. Zhu, S. Qiu, *Chem. J. Chin. Univ.* **2006**, *27*, 1194–1197.
[46] S. Park, K. Cho, M. Youn, J. Seo, J. Jung, S. Baeck, T. Kim, Y. Chung, S. Oh, I. Song, *Catal. Commun.* **2008**, *9*, 2485–2488.
[47] R. Meiers, U. Dingerdissen, W. F. Hölderich, *J. Catal.* **1998**, *176*, 376–386.
[48] A. Thangaraj, M. J. Eapen, S. Sivasanker, P. Ratnasamy, *Zeolites* **1992**, *12*, 943–950.

Received: June 8, 2009
Published Online: September 10, 2009

  